Entropy Driven Atomic Motion in Laser-Excited Bismuth

Y. Giret, A. Gellé, and B. Arnaud

Institut de Physique de Rennes (IPR), UMR UR1-CNRS 6251, Campus de Beaulieu-Bat 11 A, 35042 Rennes Cedex, France, EU

(Received 29 October 2010; published 15 April 2011)

We introduce a thermodynamical model based on the two-temperature approach in order to fully understand the dynamics of the coherent A_{1g} phonon in laser-excited bismuth. Using this model, we simulate the time evolution of (111) Bragg peak intensities measured by Fritz *et al.* [Science **315**, 633 (2007)] in femtosecond x-ray diffraction experiments performed on a bismuth film for different laser fluences. The agreement between theoretical and experimental results is striking not only because we use fluences very close to the experimental ones but also because most of the model parameters are obtained from *ab initio* calculations performed for different electron temperatures.

DOI: 10.1103/PhysRevLett.106.155503 PACS numbers: 61.80.Ba, 63.20.dk, 71.15.Pd, 78.47.J−

The development of optical pump-probe experiments has revolutionized physics by allowing the study of nonequilibrium processes on a femtosecond time scale. Indeed, an ultrashort laser pulse can cause dramatic changes in the physical properties of covalently bonded solids and induce ultrafast melting, phase transitions, or coherent phonons [1]. Coherent excitation of optical phonons is a general phenomenon which has been extensively investigated in bismuth where the reflectivity change following electronic excitations exhibits damped oscillations arising from atomic motions corresponding to the A_{1g} mode [2]. Unfortunately, it is not possible to directly relate the amplitude of the reflectivity signal to the atomic positions. The goal of measuring the atomic position as a function of time remained elusive until the breakthrough of time-resolved x-ray diffraction experiments, which allow atomic motions to be followed stroboscopically with picometer spatial and femtosecond temporal resolution [3]. Different femtosecond x-ray diffraction experiments have been conducted to probe the dynamics of the A_{1g} phonon in laser-excited Bi [4–7]. In this Letter, we try to understand and to reproduce the time evolution of (111) Bragg peak intensities measured by Fritz *et al.* [5].

Bismuth is a semimetallic solid, whose structure can be derived from the face-centered-cubic lattice by a weak rhombohedral distortion of the cubic unit cell. The crystal basis consists of two atoms located along the body diagonal of length c at $\pm uc$, where u is the A_{1g} phonon coordinate. At 300 K, the equilibrium value of u is $u_{\mathrm{eq}} \simeq 0.234$ [8]. It is now well established that the sudden change of u_{eq} following laser excitation explains the generation of coherent phonons in Bi. The time evolution of u can be obtained from the displacive excitation of coherent phonons model [2]. This model, based on the idea that u_{eq} increases linearly as a function of the excited carriers density n and that n decreases exponentially as a function of time, however, does not capture all aspects of the phonon and electron dynamics. Two approaches based on *ab initio* calculations [9,10] have been proposed to describe the nonequilibrium electron distribution. Murray *et al.* [9] assumed that electrons and holes can be described by two Fermi-Dirac distributions with the same temperature but different chemical potentials and obtained a good agreement with experiments concerning the early oscillations of the A_{1g} phonon [5]. Zijlstra, Tatarinova, and Garcia [10] studied the coupling between the A_{1g} and E_g modes and assumed that electrons and holes can be described by a unique Fermi-Dirac distribution. They claimed that a two-chemical potential model does not provide a realistic description of the electron dynamics in Bi, at least for high fluences. While such a claim seems to be supported by recent work based on a two-fluid model [6], the relevance of the two approaches remains unclear [11,12].

In this work, we consider a model based on the two-temperature approach [13] where the electron system is locally described by a single Fermi-Dirac distribution, the A_{1g} phonon mode obeys a classical equation of motion, and all the remaining modes are lumped in a unique phonon bath with specific heat C_l. We assume that both the electron temperature T_e and lattice temperature T_l are well defined at each time because of electron-electron and phonon-phonon interactions. Making a local energy balance, the heat, respectively, received by the electron and phonon systems is given by

$$T_e \frac{\partial S}{\partial t} = \frac{\partial U}{\partial t} + \frac{fc}{v}\frac{\partial u}{\partial t} = P + \frac{\partial}{\partial z}\left(\kappa_e \frac{\partial T_e}{\partial z}\right) - G_0(T_e - T_l), \tag{1}$$

$$C_l \frac{\partial T_l}{\partial t} = +G_0(T_e - T_l) + \frac{4Mc^2}{v\tau}\left(\frac{\partial u}{\partial t}\right)^2, \tag{2}$$

where P is the energy deposited by the laser pulse in the electron system per unit volume and time, S and U are electronic entropy and energy per unit volume, respectively, f is the force acting on the A_{1g} phonon, κ_e is the electron thermal conductivity, G_0 is the electron-phonon coupling constant which governs the heat transfer from the

electron system to the lattice, v is the unit cell volume, M is the mass of a Bi atom, and τ is the lifetime of the A_{1g} phonon. Since the laser spot diameter is much larger than the penetration depth, we consider only the spatial dependence of the parameters in the direction perpendicular to the surface, labeled as z. One should notice that all parameters of Eqs. (1) and (2) depend on T_e and u, both of which depend on the depth z. These equations have to be solved together with the phonon equation of motion

$$\frac{\partial^2 u}{\partial t^2} = \frac{f}{2Mc} - \frac{2}{\tau}\frac{\partial u}{\partial t}, \tag{3}$$

where the last term describes the energy transfer from the coherent phonon to the incoherent phonon bath and where the force f is defined by

$$f = -\frac{v}{c}\frac{\partial U}{\partial u}\bigg|_S. \tag{4}$$

In order to evaluate the force f acting on the coherent phonon and other quantities involved in our model, we performed *ab initio* calculations for different electron temperatures T_e and phonon coordinates u. All these calculations were done within the framework of the local density approximation for the exchange-correlation functional to density functional theory using the ABINIT code [14]. Spin-orbit coupling was included and an energy cutoff of 15 hartree in the plane wave expansion of wave functions together with a $12 \times 12 \times 12$ k-point grid for the Brillouin zone integration was used. These parameters ensure the convergence of both vibrational and electronic properties [15]. The experimental lattice parameters at room temperature are used [8], and volume changes due to an increase of the lattice temperature T_l are neglected.

First, we calculated both energy U and entropy S as a function of u and T_e and hence obtained $U(S, u)$. Figure 1(a) shows that the equilibrium position u_{eq} increases from 0.233 to 0.25 as S increases from 0 to $\sim 2.0 k_B$ per unit cell. This finding confirms the displacive mechanism of phonon generation and is qualitatively in line with the behavior observed by Murray *et al.* [9] using a two-chemical potential approach or by Zijlstra, Tatarinova, and Garcia [10] using the same type of approach as in the work reported here. If we assume that the laser pulse energy is deposited homogeneously at the end of the pulse ($\kappa_e \to \infty$), Eq. (1) shows that the electronic entropy S becomes a constant of motion provided that the energy transfer from the electron system to the lattice is frozen ($G_0 = 0$). The solution of Eq. (3) when $\tau \to \infty$ (undamped dynamics) then provides the phonon frequency ν of the A_{1g} mode for a given entropy S which depends on the laser pulse fluence. Figure 1(b) shows that ν decreases from 2.93 THz to 0 when S increases from 0 to $\sim 1.37 k_B$ per unit cell. This redshift is still in qualitative agreement with previous theoretical studies [9,10].

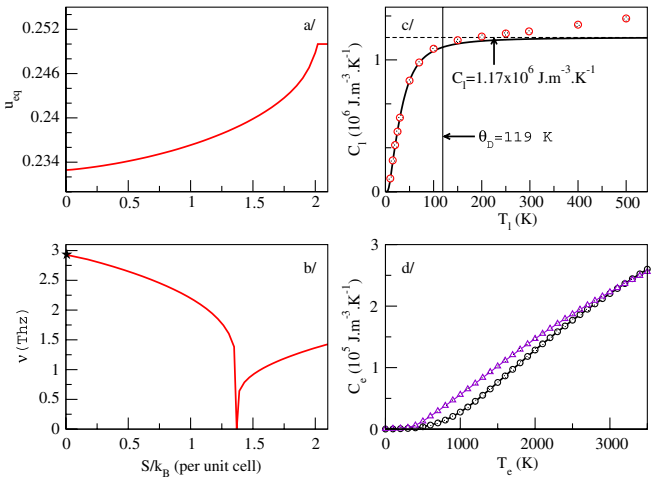

FIG. 1 (color online). (a) u_{eq} as a function of electronic entropy S. (b) A_{1g} phonon frequency ν (in terahertz) as a function of S. The star indicates the Raman frequency measured at 300 K [17]. (c) The calculated constant-volume lattice specific heat C_l (solid line) of Bi compared to experimental data (open circles) from Ref. [17] for lattice temperatures T_l up to the melting temperature $T_f = 544$ K. (d) Calculated electron specific heat C_e as a function of electron temperature T_e for $u = 0.233$ (circles) and $u = 0.24$ (triangles).

We have also calculated the lattice specific heat C_l within the harmonic approximation [16]. As shown in Fig. 1(c), the agreement between our calculated lattice specific heat and the experimental data [17] is good up to $T_l \sim 300$ K. The discrepancies between theoretical and experimental results become larger at higher temperature because of anharmonic interactions neglected in our calculation. In our simulations, the initial lattice temperature T^0 was set to 300 K. As $T^0 \gg \theta_D$, where $\theta_D = 119$ K is the Debye temperature, the temperature dependence of C_l can be neglected. Indeed, $C_l(T^0)$ is only 1% smaller than the value given by the Dulong-Petit law shown as a dashed line in Fig. 1(c). The electron temperature dependence of C_l can also be safely neglected.

Finally, we calculated the electron specific heat of Bi, $C_e = \partial U/\partial T_e$, as a function of electron temperature T_e for different values of u. As expected, the temperature dependence of C_e is linear at low electron temperatures. Figure 1(d) shows that a significant positive deviation from the linear behavior occurs when T_e becomes larger than ~ 300 K and that this deviation increases when u increases, i.e., when Bi goes toward the hypothetical metallic state corresponding to $u = 0.25$. The knowledge of $C_e(T_e)$ is crucial, not only because it gives a correct estimate of the rise of temperature in the electron system but also because it is related to the electron thermal conductivity κ_e. Indeed, assuming that the total electron scattering rate is dominated by the electron-phonon scattering rate, the electron thermal conductivity can be approximated by $\kappa_e(T_e, T_l) = \kappa_0 \times [C_e(T_e)/C_e(T^0)] \times (T^0/T_l)$ [18,19], where the

dependence on u has been omitted and where $\kappa_0 = 11\ \mathrm{W \cdot m^{-1} \cdot K^{-1}}$ is the experimental value at room temperature [20].

We can now simulate the time-resolved x-ray diffraction experiments performed by Fritz *et al.* [5] on a Bi film of thickness $L = 50$ nm excited by a near-infrared laser pulse whose FWHM is $t_w = 70$ fs. The source term $P(z, t)$ in Eq. (1) is given by

$$P(z, t) = \frac{2F_{\mathrm{abs}}}{l_p t_w}\sqrt{\frac{\ln 2}{\pi}}\exp\left[-4\ln 2\frac{t^2}{t_w^2}\right]\exp\left[-\frac{z}{l_p}\right], \quad (5)$$

where $l_p = 14$ nm is the penetration depth at a wavelength of 800 nm [17] and F_{abs} is the absorbed fluence. The solution of the coupled differential equations (1)–(3), for a set of the two unknown physical parameters G_0 and τ, which are assumed to remain constant on the time scale of the experiment for a given fluence, provides $u(z, t)$ and $T_e(z, t)$. As will be seen later, the spatial dependence of u and T_e can be neglected only ~100 fs after the arrival of the laser pulse on the Bi surface. Therefore, the normalized intensity of the (111) Bragg peak is given by $I(t)/I(0) = \cos^2[6\pi u(t)]/\cos^2[6\pi u(0)]$ and is convoluted with a Gaussian with FWHM t_X to account for the temporal resolution of the experiment [5]. The results of a least-squares fit of our model to the experimental data are shown as solid curves in Fig. 2 for four absorbed fluences. The parameters F_{abs}, G_0, τ, and t_X are given in the caption.

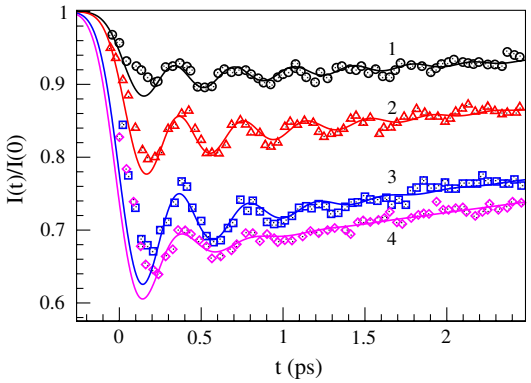

FIG. 2 (color online). Normalized intensities of the (111) Bragg peak measured by Fritz *et al.* [5] as a function of time delay t between the laser pulse and x-ray probe for different absorbed fluences (symbols) compared to the theoretical calculation (solid lines). The measured fluences are 0.7 (circles), 1.2 (triangles), 1.7 (squares), and 2.3 $\mathrm{mJ \cdot cm^{-2}}$ (lozenges). The parameters used in our simulations are given from top to bottom for curves labeled 1–4: The absorbed fluences F_{abs} are 0.64, 1.26, 2.18, and 2.47 $\mathrm{mJ \cdot cm^{-2}}$, the effective electron-phonon coupling constants G_0 are 0.84, 1.15, 1.40, and 1.45×10^{16} $\mathrm{W \cdot m^{-3} \cdot K^{-1}}$, and the decay times τ are 0.87, 0.64, 0.44, and 0.25 ps, respectively. The uncertainties for τ are quite large for curves 1 and 2 because of the limited duration of the experiments. The fitted value of the FWHM of the x-ray pulses is $t_X = 205$ fs.

The absorbed fluences used in our calculations are very close to the experimental fluences with the largest deviation occurring for the curve labeled 3 in Fig. 2. The electron-phonon coupling constant G_0 increases from 0.84 to 1.45×10^{16} $\mathrm{W \cdot m^{-3} \cdot K^{-1}}$, and the decay time τ of the coherent phonon decreases from 0.87 to 0.25 ps as the theoretical fluence increases from 0.64 to 2.47 $\mathrm{mJ \cdot cm^{-2}}$. The reported electron-phonon coupling constants are small compared to usual values in metals [18] because the density of states at the Fermi level is very small for Bi. Figure 2 shows that the oscillations of the (111) Bragg intensities are nicely reproduced by our quasi-isentropic model with the exception of curve 3, where F_{abs} is overestimated with respect to the experimental fluence. It is worth remarking that curves 3 and 4 are very close to each other while the experimental fluences differ by 0.6 $\mathrm{mJ \cdot cm^{-2}}$. Interestingly, an upward shift of curve 3 by about 0.05 leads to a better agreement with our theoretical intensity for a fluence $F_{\mathrm{abs}} = 1.79$ $\mathrm{mJ \cdot cm^{-2}}$ very close to the experimental one.

One can now discuss the physical processes playing a role in the generation of coherent phonons. The laser energy is initially deposited in the electron system since the laser pulse duration is much shorter than the characteristic time for the electron-lattice energy exchange. At the same time, the heat diffuses in the electron system. The diffusivity χ is approximately constant and given by $\kappa_0/C_e(T^0) \simeq 100\ \mathrm{cm^2 \cdot s^{-1}}$. Therefore, the usual electron heat transport occurs, and the time needed to uniformize the electron temperature T_e is roughly given by $L^2/\chi \sim 250$ fs. Our simulations show that the spatial variations of T_e, S, and u can be safely neglected only 100 fs after the laser pulse maximum. The strong overheating of the electron system at the end of the laser pulse is illustrated in Fig. 3(b). The electron temperature reaches 2231 K for the lowest fluence and 3724 K for the highest fluence. The corresponding increases of electronic entropy S are, respectively, 0.39 and $0.98k_B$ per unit cell. As shown in Fig. 1(a), the increase in entropy leads to an increase in u_{eq}. The atoms thus start to oscillate around a new equilibrium position which evolves slowly as a function of time t due to heat transfer from the electron system to the lattice. The damped oscillations of the reduced coordinate u as a function of time delay t are shown in Fig. 3(a). The initial redshift of the phonon frequency ν as the fluence increases is clearly visible and can be attributed to the decrease of ν as S increases [see Fig. 1(b)]. Figure 3 also shows that the oscillations of the phonon coordinate u are accompanied by oscillations in the electron temperature T_e whose amplitude and damping grow with fluence. The oscillations in T_e and u are in antiphase with respect to each other. Such a behavior is easy to understand if one assumes that the electron subsystem undergoes an isentropic transformation ($G_0 \rightarrow 0$). As the metallicity of Bi is enhanced when u increases, the electronic entropy S at constant electron

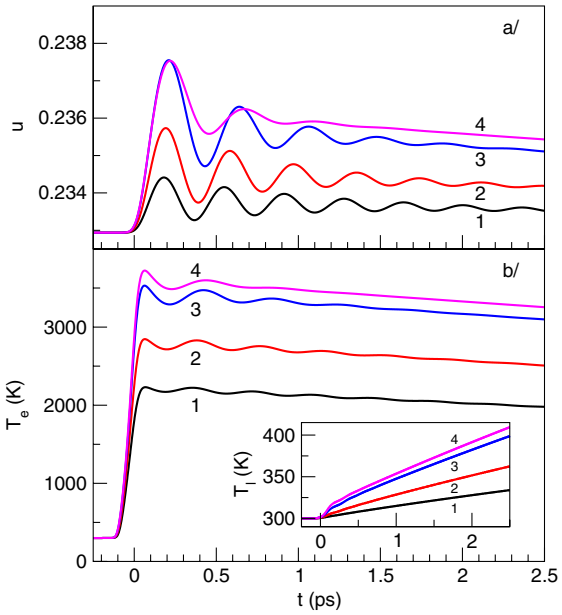

FIG. 3 (color online). (a) u as a function of time delay t for the parameters given in the caption of Fig. 2. (b) Electron temperature T_e as a function of time delay t. The inset displays the variation of the lattice temperature T_l as a function of t. The curves labeled 1–4 are related to the curves with the same label in Fig. 2.

temperature would increase up to a maximum value for the largest value of u. In order to compensate for the increase of S, T_e decreases and reaches its minimum value when u reaches its maximum value. Thus, T_e oscillates at the same frequency as u but in antiphase. Interestingly, such a behavior parallels that of a gas enclosed in an insulating piston chamber. Assuming that the gas undergoes an isentropic transformation, the piston when displaced from its equilibrium position, performs an oscillatory motion while the gas temperature undergoes a similar oscillatory motion but in antiphase. In Bi, the electronic entropy S does not remain constant after the arrival of the laser pulse but decays slowly due to energy exchange between the electron and lattice subsystems. The inset in Fig. 3(b) shows the evolution of the lattice temperature T_l as a function of time delay t. On the time scale of the experiments (~ 2.5 ps), the increase in T_l ranges from 34 K for the lowest fluence to 110 K for the highest fluence. Although the increase of the lattice temperature is significant for the highest fluence, volume changes are expected to be delayed as illustrated by the shift in the Bragg angle occurring on a time scale of $\sim$20 ps in experiments [5]. It is thus reasonable to assume that the lattice parameters remain constant in our simulations.

In conclusion, we have developed a thermodynamical model in order to simulate the time evolution of the A_{1g} phonon coordinate following the arrival of a laser pulse of a given fluence on a Bi film. The intensities of the (111) Bragg peak measured by Fritz *et al.* [5] are fairly well reproduced by our model for fluences very close to the experimental ones. This success is noteworthy since the force acting on the coherent phonon as well as most of the model parameters are obtained from *ab initio* calculations. The only adjustable parameters are the effective electron-phonon coupling constant G_0 and the scattering time $1/\tau$ of the coherent phonon. Our results show that (i) both parameters increase as the fluence increases, (ii) the electronic heat diffusion is crucial, and (iii) the oscillations of the coherent phonon are accompanied by an oscillation in the electron temperature. From a fundamental point of view, this work firmly establishes that a single chemical potential approach is reliable for describing the excited electrons and provides a complete scenario for the generation of coherent phonons in Bi films.

This work was performed by using HPC resources from GENCI-CINES (Grant 2010-095096). We thank K. Dunseath and H. Cailleau for useful comments.

[1] K. H. Bennemann, J. Phys. Condens. Matter **16**, R995 (2004).
[2] H. J. Zeiger *et al.*, Phys. Rev. B **45**, 768 (1992).
[3] T. Pfeifer, C. Spielmann, and G. Gerber, Rep. Prog. Phys. **69**, 443 (2006).
[4] K. Sokolowski-Tinten *et al.*, Nature (London) **422**, 287 (2003).
[5] D. M. Fritz *et al.*, Science **315**, 633 (2007).
[6] S. L. Johnson *et al.*, Phys. Rev. Lett. **100**, 155501 (2008).
[7] S. L. Johnson *et al.*, Phys. Rev. Lett. **102**, 175503 (2009).
[8] D. Schiferl and C. S. Barrett, J. Appl. Crystallogr. **2**, 30 (1969).
[9] E. D. Murray, D. M. Fritz, J. K. Wahlstrand, S. Fahy, and D. A. Reis, Phys. Rev. B **72**, 060301 (2005).
[10] E. S. Zijlstra, L. L. Tatarinova, and M. E. Garcia, Phys. Rev. B **74**, 220301 (2006).
[11] E. S. Zijlstra, L. E. Díaz-Sánchez, and M. E. Garcia, Phys. Rev. Lett. **104**, 029601 (2010).
[12] S. L. Johnson *et al.*, Phys. Rev. Lett. **104**, 029602 (2010).
[13] M. I. Kaganov, I. M. Lifshitz, and L. V. Tanatarov, Zh. Eksp. Teor. Fiz. **31**, 232 (1956); [Sov. Phys. JETP **4**, 173 (1957)].
[14] X. Gonze *et al.*, Comput. Phys. Commun. **180**, 2582 (2009).
[15] L. E. Díaz-Sánchez, A. H. Romero, and X. Gonze, Phys. Rev. B **76**, 104302 (2007).
[16] L. E. Díaz-Sánchez, A. H. Romero, M. Cardona, R. K. Kremer, and X. Gonze, Phys. Rev. Lett. **99**, 165504 (2007).
[17] *American Institute of Physics Handbook*, edited by D. E. Gray (McGraw-Hill, New York, 1972), 3rd ed.
[18] Z. Lin, L. V. Zhigilei, and V. Celli, Phys. Rev. B **77**, 075133 (2008).
[19] A. P. Kanavin *et al.*, Phys. Rev. B **57**, 14 698 (1998).
[20] C. F. Gallo, B. S. Chandrasekhar, and P. H. Sutter, J. Appl. Phys. **34**, 144 (1963).